Optics Communications 100 (1993) 443–450
North-Holland

OPTICS
COMMUNICATIONS

Laser induced dynamics of atomic sublevel coherences

Dieter Suter and Thomas Marty
Institute of Quantum Electronics, Swiss Federal Institute of Technology (ETH) Zürich, CH-8093 Zürich, Switzerland

Received 16 December 1992; revised manuscript received 25 February 1993

In atomic media, the interaction with resonant light leads to optical pumping and light shift effects which modify not only the static optical and magneto-optical properties of the media, but also the dynamics of multipole moments that are present in the electronic ground state as well as in electronically excited states. These modified dynamics include changes in precession frequencies and relaxation rates, but also laser-induced exchange of coherences between different atomic multipole moments. Using the Na ground state as an example, a theoretical analysis of these modified dynamics is presented, as well as experimental measurements of the laser induced coherence transfer.

1. Introduction

The resonant interaction of light with atomic systems can create anisotropic states in the atomic medium by transferring angular momentum from the photons to the atomic medium [1]. If the interaction excites such states in the electronic ground state, they can have a very long lifetime and the corresponding media tend therefore to exhibit highly nonlinear optical properties even at low laser intensities. The exchange of angular momentum between photons and atoms not only creates these anisotropic states, but also leads to "displacement and broadening of magnetic resonance transitions", effects which were first observed and explained by Barrat and Cohen-Tannoudji [2]. The interaction with the light thus drives the system away from its equilibrium position and thereby affects the way in which the medium interacts with its environment. The linear, and especially the nonlinear magnetooptical effects [3,4] are a manifestation of such anisotropic atomic states. In addition, processes of this type are responsible for sub-Doppler laser cooling and trapping of neutral atoms [5]. Even more recently, they have been found to play an essential role in the magneto-optic force, a strong, non-saturating, light-induced force that acts on atoms coupled to strong laser fields in the presence of magnetic fields [6].

These are some of the effects that the coupling between atoms and optical radiation has on the static properties of the atomic medium. However, the radiation affects not only the equilibrium properties, but also the dynamic behaviour of atomic multipole moments. As an example, the light shift effect of a laser pulse can reverse the dephasing of spins undergoing Larmor precession in an inhomogeneous magnetic field [7]. This experiment shows that light shift and damping effects modify the precession frequencies and relaxation rates of the multipole moments. While effects of this type can be attributed to changes in the eigenvalues of the effective hamiltonian, the coupling between light and atomic media can also change the quantization direction of the hamiltonian. Such a rotation of the quantization axis of the effective hamiltonian causes the lifting of the zero field Zeeman degeneracy observed in optical-radiofrequency double resonance experiments [8] and can induce the transfer of sublevel coherence among different orders of atomic multipole moments [9].

In this communication, we present the first analysis of such dynamic effects in an electronic ground state that consists of more than two energy levels. We consider the $3s\,^2S_{1/2}$ electronic ground state of atomic sodium with eight angular momentum substates that are split into two hyperfine multiplets with total angular momentum $F=1$, 2. In principle, the optical excitation process can prepare the atomic

system in arbitrary superpositions of the Zeeman substates. The conventional expansion of the resulting atomic state uses atomic multipole moments as the basis operators [10]. In the case of the Na ground state, it is possible to excite moments up to hexadecupoles ($\Delta m = \pm 4$); these atomic multipole moments evolve under the influence of the atomic hamiltonian as well as the coupling to external fields. In our experiment, we use optical pumping in a transverse magnetic field to create the multipole moments and a second laser beam for monitoring the resulting dynamics.

Optical observation of atomic multipoles is possible for dipole and quadrupole moments [11], i.e. orientation and alignment. While the optical detection does not observe the higher order moments directly, optical pumping does excite these moments, and it is possible to infer their existence from indirect evidence [12]. Under suitable conditions, laser excited coherence transfer processes can convert the "invisible" higher order moments into directly observable dipole moments. They can therefore form the basis of an experiment that permits the indirect observation of "forbidden" Raman transitions [13]. Using such experiments, it is in principle possible to reach a complete characterization of resonant atomic multilevel systems, even when they are too complex to be studied by conventional methods. It is of course possible to perform such experiments without a detailed knowledge of the mechanisms that cause the coherence transfer process. However, an improved understanding of these mechanisms is not only of fundamental interest, it is also a necessary prerequisite for optimising experimental procedures. This is the purpose of this letter: we describe the basics of the physical processes that cause these coherence transfer processes.

For a theoretical analysis of the static magnetooptic properties of such a system, it is often possible to use perturbation methods. These methods lead to a description of the system, which is adequate if the optical interaction is small, driving the system not too far from thermal equilibrium. For our discussion of dynamical effects, such a perturbation analysis is not possible. Since an analytical solution to the equations of motion for this full system is not possible, we can only treat certain aspects analytically and must resort to numerical methods for the full dynamics. In the present context, we emphasise the evolution of the atomic system under the influence of the laser irradiation. For the discussion of related topics, such as the effect of the order in the system on the optical fields [9,13,14], and the experimental aspects [14,15], we refer to the literature.

2. Theory

In the present context, we discuss atomic multipole moments in the electronic ground state of atomic sodium. Figure 1 shows a schematic representation of the level scheme of the Na D_1 transition. The quantization axis is parallel to the magnetic field so that the states represent eigenstates of the hamiltonian in the absence of light. We start the analysis of the system with the dynamics induced by an external magnetic field. The Zeeman interaction between the external magnetic field B and the total angular momentum F of the atomic system is then

$$\mathcal{H}_Z = \sum_{i=1}^{2} g_{Fi} B F_z^{(i)} + g_{Fi}^{(2)} B^2 F_z^{(i)2}, \qquad (1)$$

where the index i runs over the two hyperfine multiplets. g_{Fi} and $g_{Fi}^{(2)}$ are the Zeeman coupling constants for the linear and quadratic Zeeman interaction; approximate numerical values for the Na ground state are $g_{Fi} = 7$ MHz/mT and $g_{Fi}^{(2)} = 27$ kHz/mT^2;

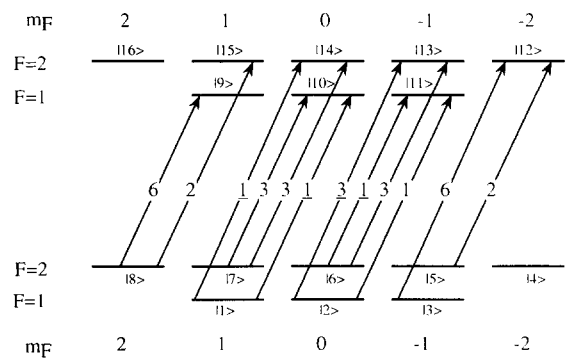

Fig. 1. Level scheme of the Na ground state. The individual levels are labelled with the quantum number (F, m_F) and a running index starting at the lowest energy level. The arrows indicate optical transitions for circularly polarized light propagating in the direction of the quantization axis and the numbers indicate the dipole matrix elements for these transitions.

the nuclear Zeeman effect is included in a modified g_{F_i}. $F_z^{(i)}$ is the z-component of the total angular momentum in the hyperfine multiplet i. With these assumptions, the evolution of the system corresponds to a phase accumulation of the off-diagonal density operator elements

$$\rho_{ij}(t)=\rho_{ij}(0)\exp(i\omega_{ij}t)\,, \tag{2}$$

where $\omega_{ij}=(E_j-E_i)/\hbar$ represents the precession frequency of transition ij. With our experimental setup, which we discuss in the next section, it is possible to observe those density operator elements that connect eigenstates differing by $\Delta m=\pm 1$. Fourier transformation of the time-domain data allows a separation of the different elements through the different precession frequencies ω_j, as shown in fig. 2. The labels of the form $(F, m_F \leftrightarrow F', m_{F'})$ assign the six resonance lines appearing in this figure to transitions between the corresponding angular momentum states. The origin of the frequency axis corresponds to the reference frequency of the phase sensitive detector [15], to allow direct comparison with the experimental data.

For the discussion of the optical effects, we assume that the laser intensity is well below the saturation intensity of the optical transition; we may then neglect the excited state populations. Furthermore, we neglect Doppler broadening. In the experiment, we satisfy both conditions by using buffer gas to achieve a homogeneous, pressure broadened optical resonance line. Figure 1 shows the possible transitions between ground state sublevels and angular momentum states of the $^2P_{1/2}$ excited state. The arrows indicate those transitions, which couple to circularly polarised light propagating along the quantization axis. The numbers close to the arrows indicate the squares of matrix elements of the electric dipole matrix elements; underscores indicate negative matrix elements. Each of these transitions contributes to the optical pumping and light shift effects.

We start with the calculation of the rates for depopulation pumping [15]. The loss of population from level i due to optical pumping is $\dot{\rho}_{ij}(t)=-k_i\rho_{ij}(t)$, where k_i is the depopulation pumping rate for the ground state sublevel i. We express the individual rates in terms of the constant

$$k_0=\frac{{E_0}^2 d^2}{8\hbar^2\Gamma_2}\frac{1}{1+(\Delta/\Gamma_2)^2}\,, \tag{3}$$

where E_0 is the amplitude of the optical field, d the reduced dipole moment, Γ_2 the optical dephasing rate, and $\Delta=\omega_{las}-\omega_0$ the detuning of the laser frequency ω_{las} from the atomic resonance frequency ω_0. The individual rates are determined by the squares of the dipole matrix elements. As shown in fig. 1, the individual rates k_i for levels $i=1...8$ are

$$(k_1, k_2, ..., k_8)=k_0(1, 2, 3, 0, 1, 2, 3, 4)\,. \tag{4}$$

We calculate the repopulation rate from the conservation of the total population. Assuming fast reorientation in the excited state, the equation of motion for the ground state populations is then

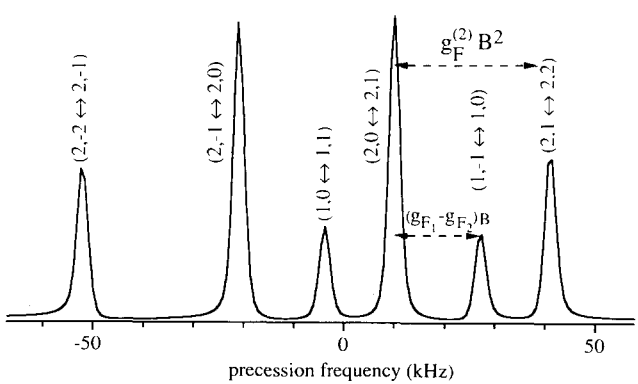

Fig. 2. Calculated sublevel spectrum of the Na ground state in a magnetic field $B=0.7$ mT. The six resonance lines correspond to six density matrix elements which are identified in the figure, using the notation $(F, m_F \leftrightarrow F', m_{F'})$.

$$\dot{\rho}_{ii}(t) = -k_i\rho_{ii}(t) + \frac{1}{8}\sum_{i=1}^{8} k_i\rho_{ii}(t) \,. \quad (5)$$

Coherences ρ_{ij} between the ground state sublevels experience light shift and damping effects [2,15]:

$$\dot{\rho}_{ij}(t) = -(\gamma_{ij} - i\delta_{ij})\rho_{ij}(t) \,, \quad (6)$$

with

$$\gamma_{ij} = (k_j + k_i)/2, \quad \delta_{ij} = \Delta/\Gamma_2(k_j - k_i) \,. \quad (7)$$

The light shift effect is therefore equivalent to a magnetic field in laser beam direction. In general, light shift effects contain also contributions corresponding to electric quadrupole fields [2]. However, since we have neglected the hyperfine splitting of the excited state, these effects do not appear in this system. Physically, this difference arises from collisions of the atoms with the buffer gas that lead to a pressure broadening much bigger than the excited state hyperfine splitting. These collisions cause also a rapid reorientation of the excited state atoms. The damping of the sublevel coherences, described by γ_{ij}, is highest for coherences with the highest depopulation pumping rates. Since we can describe the evolution of the system in a reference frame whose quantization axis is parallel to the laser beam direction, the optical effects alone do not lead to a mixing of the different multipole moments.

In the case of modulated excitation [15,16], the same equations of motion as in the laboratory frame determine the evolution in the rotating frame, if the optical pumping rate and the light shift effect are reduced by a factor that depend on the modulation scheme and is of the order of 1/2. In addition, there is always a contribution that corresponds to the opposite polarisation and increases the effective damping rate for the optical pumping process as well as for the coherences. As discussed elsewhere, the effective magnetic field in this reference frame is reduced by an amount proportional to the modulation frequency [15]; as a result, the coherences evolve at the difference between the Larmor and the modulation frequencies.

With magnetic or optical effects alone acting on the atomic system, it is possible to describe the sublevel dynamics in a relatively straightforward way in a reference frame that takes the respective symmetries into account. In our experiment, we apply a magnetic field perpendicular to the laser beam. Under these conditions, no such symmetry-adapted coordinate system exists. We must therefore express the equation of motion in one of the two coordinate systems used above. For this purpose, we use a reference frame whose quantization axis is parallel to the magnetic fields. In this coordinate system, the optical pumping process creates no longer only diagonal, but also off-diagonal density operator elements. Figure 3 shows the creation of atomic multipole moments. We have calculated these curves by numerically integrating the equations of motion, assuming modulated optical pumping in a transverse magnetic field. For this purpose, we have transformed the equations of motion into a frame of reference rotating around the magnetic field at the modulation frequency [15]. The solutions represent therefore slowly varying amplitudes that do not include the fast Larmor precession around the magnetic field (at 5.2 MHz in our case), but only the slow Larmor precession in a reduced magnetic field $B_{\text{eff}} = B_0 - \omega_{\text{mod}}/g_F$. For the calculation, we have chosen a magnetic field strength $B_0 = 0.7$ mT, a laser intensity of 90 mW/mm^2 and a laser detuning $\Delta/2\pi = 12$ GHz. The four curves in fig. 3 show the resulting time-dependence of density operator elements corresponding to different atomic multipoles. Clearly, the optical pump-

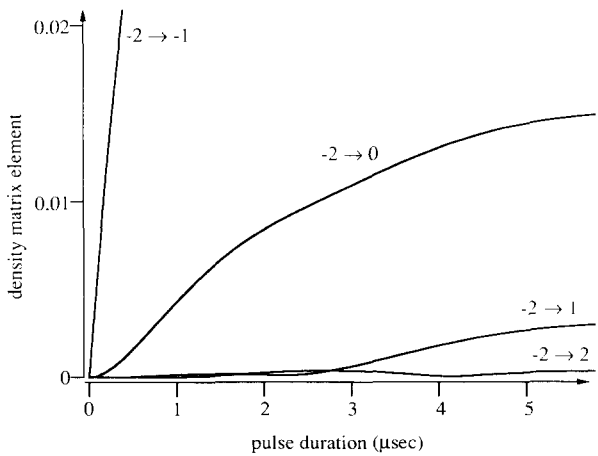

Fig. 3. Amplitude of selected density operator elements plotted as a function of time during optical pumping. The system is initially in thermal equilibrium and the curves show the creation of various atomic multipoles.

ing in the presence of the transverse magnetic field excites all possible multipoles.

The equations of motion derived here describe the evolution of this system during optical pumping. If the system is initially in thermal equilibrium, as we have assumed for the curves of fig. 3, they describe therefore the *creation* of sublevel coherences. If, on the other hand, the system is already in an anisotropic state, the resulting process includes in addition an *exchange* of coherence between different multipoles. Figure 4 demonstrates this process for the same conditions as in fig. 3: the curves represent the amplitude of four density operator elements as a function of time while a pump laser pulse drives the system. For this calculation, we assumed that the system is initially in a coherent superposition of the angular momentum substates $(F, m_F) = (2, -2)$ and $(2, -1)$. The curves in fig. 4 represent the amplitude of the density operator elements that correspond to transitions between neighbouring angular momentum substates. The laser pulse apparently causes a transfer of coherence among the different sublevel transitions. The combined effect of light shift and Zeeman interaction lead to the oscillatory evolution, while the damping effect of the laser field is largely responsible for the overall decay.

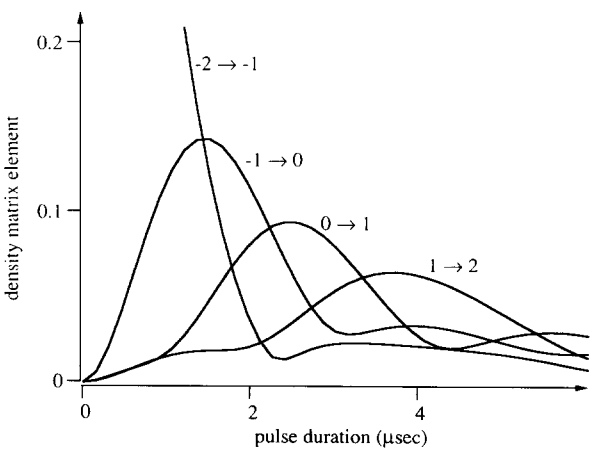

Fig. 4. Amplitude of selected density operator elements plotted as a function of time during optical pumping. For $t=0$, the only nonvanishing density operator element corresponds to the $(2, -2 \leftrightarrow 2, -1)$ transition. The curves show the laser-induced transfer of coherence from this density matrix element to other multipoles.

3. Experiments

For a comparison of this theoretical analysis with experimental data, we used the setup of fig. 5. The measurements reported here were performed on the $3s\ ^2S_{1/2}$ sodium ground state. The atomic vapour was contained in a 1 cm long glass cell at a temperature of 200 °C, together with 200 mbar of Ar buffer gas. The pressure broadening of 4 GHz (fwhm) produced a homogeneous optical resonance line. The light source was a single-mode cw ring dye laser with a short term linewidth less than 500 kHz. The laser frequency was set near the Na-D_1 line ($\lambda = 589.6$ nm) with a detuning $\Delta = 12$ GHz above the centre of the (pressure-shifted) resonance line, in a region where the light shift effect exceeds the damping effect. The laser beam was split into a pump beam with an intensity of ~ 150 mW/mm^2 and a probe beam with an intensity ~ 0.6 mW/mm^2, which overlapped in the sample region at an angle of less than 1°. The laser pulses were generated by an acousto-optic modulator (AOM) driven by a computer-controlled digital delay generator. The transverse magnetic field of 0.7 mT caused a well-resolved quadratic Zeeman effect, as shown in fig. 2. In a transverse magnetic field of this size, cw optical pumping is of course rather inefficient. Therefore, we modulated the polarization of the laser beam between opposite circular polarizations to enhance the effects that we wanted to study. This modulation [15,16] leads to a resonant enhancement of the optical pumping effects when the modulation frequency matches the Larmor frequency of the system. As discussed in the theoretical

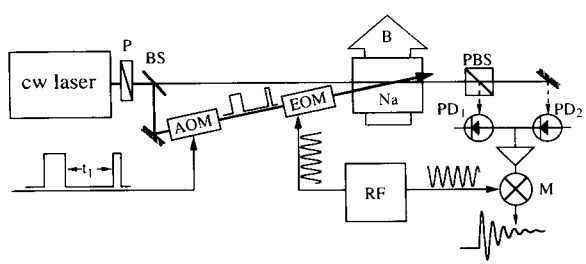

Fig. 5. Schematic representation of the experimental setup. P: polarizer, BS: beam splitter, AOM: acoustooptic modulator, EOM: electrooptic modulator: rf: radio-frequency synthesizer, B: magnetic field, PBS: polarizing beam-splitter, $PD_{1,2}$: photodiodes, M: mixer.

section, the time scale for the evolution of the coherences is determined by the difference between the Larmor and modulation frequencies. Therefore, we had to control the shape of the laser pulses only on a timescale $\tau > 1$ μs [15].

In the experiment, a first pump laser pulse creates the sublevel coherences whose dynamics we wish to investigate. After the pulse, the system evolves in the magnetic field alone. During this free precession period, the multipole moments accumulate a phase that depends on the precession frequency and therefore on the strength of the magnetic field. By choosing an appropriate field strength, this allows us to uniquely identify the individual multipole moments or to prepare an arbitrary initial state of the system. With the coherences labelled this way, we then apply a second laser pulse that induces the dynamics that we wish to study. We monitor these dynamics by letting the system evolve freely again for a second time after the end of the laser pulse. Like the first evolution period, this second free precession period allows an identification of the individual sublevel coherences, this time after the pulse. We monitored this evolution with a linearly polarized probe laser beam that measured the circular birefringence of the sample. Before digitisation, the resulting signal was down converted with a double-balanced mixer, using the modulation frequency as the local oscillator [15].

For an efficient analysis of the data, we measured the response of the system as a function of the two free precession times and subsequently Fourier transformed the data with respect to both time variables. In the resulting two-dimensional spectrum, every signal contribution is identified by two resonance frequencies that correspond to the precession frequencies during the two "dark" evolution periods, i.e. before and after the second laser pulse. Figure 6 shows an example of a resulting spectrum, together with the theoretical data that we obtained by numerically integrating the equations of motion (2), (5)–(7) for the system, starting from thermal equilibrium. For this experiment, the duration of the second laser pulse was 3 μs. The horizontal axis, labelled ω_2, corresponds to the precession frequency after the second pulse, while the vertical axis, labelled ω_1, represents the precession frequency between the two laser pulses. Without a second laser pulse, the atomic multipoles would of course precess at the same frequency during the two free evolution periods and all resonance lines would appear on the diagonal, where $\omega_1 = \omega_2$. The mixing of the different multipole moments by the laser pulse, however, transfers coherences from one sublevel transition to another, thereby changing the precession frequency. In the spectrum, the so-called cross peaks with $\omega_1 \neq \omega_2$ are evidence for these processes: each of these resonance lines corresponds to a different laser induced coherence transfer process. By measuring such spectra as a function of the duration of the second laser pulse, it is possible to monitor the laser induced coherence transfer processes directly.

For a comparison between the theoretical and experimental spectra, it is necessary to consider the effect of the spatial dependence of the pump laser intensity. This inhomogeneity affects the light shift as well as the damping effect. In the calculations, we have taken this into account by averaging the result over a range of laser intensities. We do not, however, expect a quantitative agreement between the theoretical and the experimental spectrum; this would require a much more elaborate analysis, taking not only the transverse profiles of both laser beams into account, but also the spatial overlap between the two beams, the reduction of the laser intensity by absorption as the beams propagate through medium, a more detailed treatment of diffusion processes, and nonlinear effects, such as radiation trapping or self-focussing processes.

4. Conclusion

To summarise, we have presented a theoretical description of the resonant interaction of polarized light with multilevel atomic media that includes not only the static, but also the dynamic effects of the coupling between the light and the atomic medium; our model includes magnetic as well as optical effects. Our main goal was an improved understanding of the recently discovered laser induced coherence transfer processes. We have sketched the equations of motion of the system, including optical pumping, light shift and magnetic effects. We have found, that the laser induced coherence transfer process can be traced to the change of the quantization axis of the effective hamiltonian: the magnetic and optical part

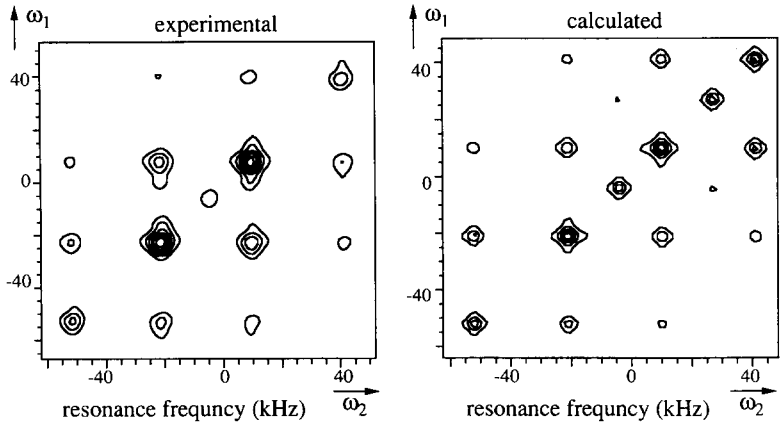

Fig. 6. Comparison of measured (left) and calculated (right) 2D spectra. Each resonance line shows the transfer of coherence between two different sublevel transitions.

of the total hamiltonian are quantized in different directions. The quantization of the effective hamiltonian changes therefore whenever the laser intensity changes. We have verified this conclusion through the comparison of a theoretical spectrum, obtained by numerical integration of these equations of motion, with experimentally measured data. The theoretical and experimental data show qualitatively the same behaviour, including the overall time scale. On the experimental side, we attribute the remaining differences primarily to an incomplete control over experimental parameters, e.g. the inhomogeneous profiles of the two laser beams; on the theoretical side, our model does not include diffusion effects or nonlinear optical effects like radiation trapping or self focusing.

For our experimental data, we have used the electronic ground state of atomic sodium, which is frequently used as a model system for magnetooptic experiments. The corresponding theoretical models treat in most cases only the static properties of the system, using perturbation theory to describe situations close to thermal equilibrium. No analysis of the dynamics of this system has, up to now, taken the effects of the nuclear spin into account. We consider the results as evidence that it is now possible to investigate even such relatively complicated systems in detail.

Two-dimensional spectroscopy represents an important tool for the experimental investigation of these dynamics. The strength of this method lies in the possibility to observe the laser induced dynamics directly and distinguish the many possible processes by separating the corresponding signal contributions in two independent frequency dimensions. In the present context, it is a prerequisite for following the coherence transfer process: it permits the identification of the multipole moments before and after the transfer process.

Acknowledgements

This work was supported by the Schweizerischer Nationalfonds.

References

[1] A. Kastler, Science 158 (1967) 214.
[2] J.P. Barrat and C. Cohen-Tannoudji, J. Phys. Rad. 22 (1961) 329, 443.
[3] S. Giraud-Cotton, V.P. Kaftandjian and L. Klein, Phys. Rev. A 32 (1985) 2211.
[4] K.H. Drake, W. Lange and J. Mlynek, Optics Comm. 66 (1988) 315.
[5] A. Aspect, E. Arimondo, R. Kaiser, N. Vansteenkiste and C. Cohen-Tannoudji, Phys. Rev. Lett. 61 (1988) 826.
[6] R. Grimm, V.S. Letokhov, Y.B. Ovchinnikov and A.I. Sidorov, J. Phys. II 2 (1992) 593.
[7] M. Rosatzin, D. Suter and J. Mlynek, Phys. Rev. A 42 (1990) 1839.
[8] J. Dupont-Roc, N. Polonsky, C. Cohen-Tannoudji and A. Kastler, Phys. Lett. A 25 (1967) 87.

[9] D. Suter, M. Rosatzin and J. Mlynek, Phys. Rev. Lett. 67 (1991) 34.
[10] A. Omont, Progr. Quantum Electron. 5 (1977) 69.
[11] S. Pancharatnam, Phys. Lett. A 27 (1968) 509.
[12] M. Ducloy, M.P. Gorza and B. Decomps, Optics Comm. 8 (1973) 21.
[13] D. Suter and H. Klepel, Europhys. Lett. 19 (1992) 469.
[14] D. Suter and J. Mlynek, Adv. Magn. Opt. Reson. 16 (1991) 1.
[15] D. Suter and J. Mlynek, Phys. Rev. A 43 (1991) 6124.
[16] H. Klepel and D. Suter, Optics Comm. 90 (1992) 46.